

Chemical Heterogeneity and Metasomatism in the Upper Mantle: Evidence from Rare Earth and Other Elements in Apatite-Rich Xenoliths in Basaltic Rocks from Eastern Australia

Suzanne Y. Wass, P. Henderson and C. J. Elliott

Phil. Trans. R. Soc. Lond. A 1980 **297**, 333-346

doi: 10.1098/rsta.1980.0219

Email alerting service

Receive free email alerts when new articles cite this article - sign up in the box at the top right-hand corner of the article or click [here](#)

To subscribe to *Phil. Trans. R. Soc. Lond. A* go to: <http://rsta.royalsocietypublishing.org/subscriptions>

Chemical heterogeneity and metasomatism in the upper mantle: evidence from rare earth and other elements in apatite-rich xenoliths in basaltic rocks from eastern Australia

BY SUZANNE Y. WASS,[†] P. HENDERSON[‡] AND C. J. ELLIOTT[‡]

[†] *School of Earth Sciences, Macquarie University, North Ryde, N.S.W. 2113, Australia*

[‡] *Department of Mineralogy, British Museum (Natural History),
Cromwell Road, London SW7 5BD, U.K.*

[Plate 1]

Apatite-rich inclusions in some basaltic rocks from eastern Australia are interpreted as mantle crystallization products of a carbonatitic/kimberlitic fluid enriched in low atomic number rare earth elements (l.r.e.e.), and are *a priori* evidence for mantle heterogeneity. The chondrite-normalized rare earth abundances of separated apatite, clinopyroxene, amphiboles and micas are high, with La in apatite being up to 4600 times chondrite. Apatites show a significant variation in rare earth content and in La:Lu ratios, indicating the occurrence of some crystal fractionation. The absence of europium anomalies from all mineral phases is indicative of a relatively high oxygen fugacity for the parent magma. The nature of the rare earth element distribution between mineral pairs suggests that some xenoliths represent equilibrium assemblages while some of the amphibole-bearing ones do not. The fluid from which these xenoliths crystallized would be an ideal agent for the metasomatism of upper mantle material and may account for l.r.e.e. enriched patterns of primary magmas in some alkaline provinces.

INTRODUCTION

Apatite-rich xenoliths are particularly abundant in a nepheline basanite dyke from Kiama, N.S.W., and also occur in nearby dykes, flows and sills. These xenoliths form a mineralogically diverse suite termed the amphibole/apatite suite by Wass (1979*a*) and are quite distinct from Cr-diopside and Al-augite suite xenoliths (Wilshire & Shervais 1975) and crustal rocks occurring in the same host basanite. They are considered to be of upper mantle origin because minerals of the amphibole/apatite suite occur as veins in, and alteration products of, associated Cr-diopside and Al-augite series xenoliths. In addition, the Ca-Tschermak's component of the constituent clinopyroxenes (Aoki & Shiba 1973; Wass 1979*b*) and the high MgO content of the ilmenite are compositional indicators of a high-pressure origin. The Ti:Al ratio (Best 1974) of the kaersutites is also consistent with high-pressure derivation. Furthermore, the world-wide association of amphibole/apatite suite minerals accompanying other high-pressure inclusions in alkali basaltic rocks, as detailed below, provide indirect supporting evidence. Such a ubiquitous association must derive from a common cause, possibly through metasomatism of the underlying mantle by l.r.e.e.-enriched fluids before partial melting.

The mineral assemblages of amphibole/apatite suite xenoliths are fully described in Wass (1979*a*) and Wass & Rogers (1980). They range from the most common xenolith type of amphibole, apatite, clinopyroxene and spinel with accessory mica, ilmenite, sulphides,

[197]

carbonate and olivine to monomineralic varieties such as spinel or apatite or amphibole xenoliths. The whole rock analyses (Wass & Rogers, unpublished data) show kimberlitic r.e. patterns and abundances, which are consistent with the interpretation (Wass 1979 *a*) that these xenoliths are crystallization products of a fractionated kimberlitic/carbonatitic magma. The characteristics of this fluid include depletion in the elements Mg, Cr and Ni, and enrichment in Fe and incompatible elements including P, Ti and r.e.e. Sequential Fe enrichment can be found among xenoliths and from layer to layer within xenoliths, indicating fractional crystallization.

The aims of the present study are:

- (1) to characterize the r.e.e. and selected trace element concentrations for separated minerals from individual xenoliths of the amphibole/apatite suite;
- (2) to assess the significance of mineral-liquid partition coefficients as applied to these xenoliths;
- (3) to establish partition coefficients of elements for existing mineral pairs;
- (4) to provide evidence of metasomatic processes and chemical inhomogeneity within the upper mantle;
- (5) to evaluate the possible relation between metasomatic events in the upper mantle and continental alkaline volcanism.

TEXTURAL EVIDENCE FOR MANTLE METASOMATISM

The Cr-diopside and Al-augite series xenoliths in the Kiama dyke are inferred to be accidental upper mantle samples (Wilshire & Shervais 1975; Irving 1980). The amphibole/apatite suite minerals commonly occur as veins or as discrete interstitial grains in, or as partial replacement or alteration of, original phases in the Cr-diopside and Al-augite series xenoliths. The most common veining minerals are amphibole, mica and apatite. Figure 1 shows development of bladed amphibole crystals in an original Al-augite series xenolith. Oxidation of the original clinopyroxene accompanies the new growth of amphibole which forms euhedral to subhedral crystals. The amphibole laths commonly include relics of original clinopyroxene and spinel grains. The minerals most commonly effecting replacement are Fe-rich clinopyroxene, amphibole and carbonate. Both original Al-augite and Cr-diopside may be partly replaced by green, Fe-rich clinopyroxene compositionally identical to that in the amphibole/apatite suite xenoliths (e.g. K24 clinopyroxene, table 1). Carbonate pseudomorphs after olivine occur (figures 2 and 3) and are accompanied by formation of oxide concentrations and also by fine-scale exsolution of ilmenite(?) plates in associated clinopyroxene. A very common but ambiguous texture is shown in figure 4. Amphibole compositionally identical to that in the amphibole/apatite xenoliths, is intergrown with Al-augite. This may simply represent coeval intergrowths or may suggest replacement of large Al-augite series clinopyroxenes by subsequent amphibole. A replacement origin is favoured because of the occurrence of irregular and complex zoning of the associated clinopyroxene, which indicates alteration to a more Fe-rich composition (although not to the extremely Fe-rich green type). The more Mg-rich areas may represent the original composition before metasomatic alteration and growth of amphibole. Evidence for this is provided by the *Mg* value (i.e. the concentration ratio $Mg/(Mg + Fe^{2+})$, by mass) of coexisting amphiboles and clinopyroxenes. Amphiboles and clinopyroxenes in textural equilibrium in the amphibole/apatite xenoliths have *Mg* values lying along the

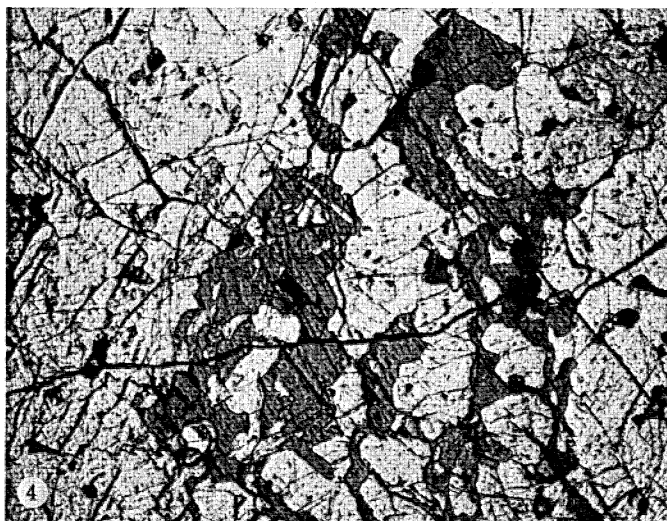
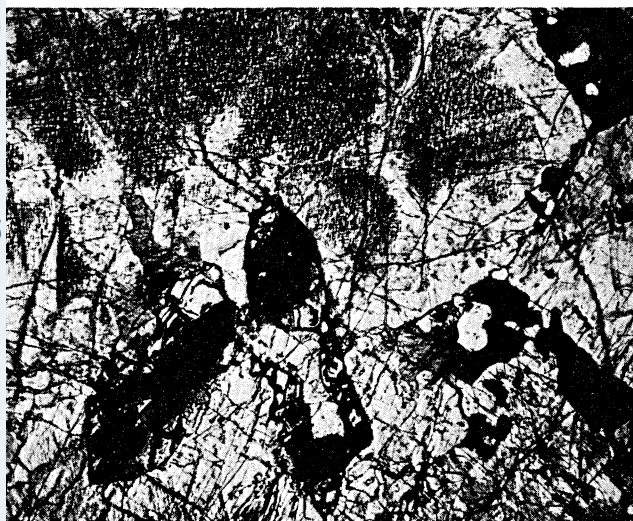


FIGURE 1. Bladed amphibole and apatite replacing clinopyroxene from original Al-augite type xenolith. Width of field of view: 3.5 mm.

FIGURE 2. Altered Al-augite type xenolith. Olivine is pseudomorphed by carbonate, original clinopyroxene is clouded with opaques and altered to Fe-rich clinopyroxene at grain boundaries. Width of field of view: 3.5 mm.

FIGURE 3. Altered Al-augite type xenolith showing altered olivine and clinopyroxene. Width of field of view: 3.5 mm.

FIGURE 4. Intergrowth of amphibole and clinopyroxene. Width of field of view: 3.5 mm.

regression line in figure 5. *Mg* values of the Mg-rich areas of zoned clinopyroxenes, when plotted against associated amphibole, give points that are displaced off the line towards higher clinopyroxene *Mg*.

These veining and replacement textures are similar to those described by Lloyd & Bailey (1975) in nodules from the Eifel region and southwest Uganda. The secondary mineral assemblages of Fe-rich clinopyroxene, amphibole, apatite, mica, spinel and carbonate from the Eifel nodules are also similar to those of the amphibole/apatite suite from Kiama. The patchy distribution of the secondary minerals, their common occurrence as monomineralic bands, and the complex zoning of clinopyroxenes from the Eifel nodules, are duplicated at Kiama. Lloyd & Bailey (1975) suggest that where the secondary hydrous phases and clinopyroxene coexist in veins and lenses in original nodules that a common high pressure origin of host rock and vein assemblages is the most likely explanation.

Kaersutitic and pargasitic amphibole is a common associate of mantle-derived inclusions in alkali basaltic rocks. Best (1974) has summarized modes of occurrence, two of which are as vein and interstitial grains in Cr-diopside series xenoliths. Amphibole, with or without clinopyroxene, mica and apatite, is also found as veins in periodotite massifs (Conqu  r   1971; Embey-Isztin 1976) and as discrete xenoliths in many alkali basaltic rocks (see, for example, Vinx & Jung 1978; Becker 1977; Best 1974, 1975; Wilshire & Trask 1971).

Xenoliths with assemblages closely comparable with those of the amphibole/apatite suite are now being recognized from many provinces of alkaline volcanism. Fe-rich clinopyroxene occurs in at least six provinces from the Cainozoic basaltic chain of eastern Australia (Wilkinson 1975; Wass & Irving 1976; Wass, unpublished data) as well as in Antarctica (Wass, unpublished data) where it is associated with kaersutite and spinel. Fe-rich, green clinopyroxene-apatite-spinel xenoliths and amphibole-Fe-rich clinopyroxene-spinel xenoliths occur associated with Cr-diopside and Al-augite series inclusions from the Massif Central (Wass 1979*b*; Babkine *et al.* 1968). Kaersutite-bearing inclusions with or without apatite and clinopyroxene (green, Fe-rich) are recorded from the Eifel region (see, for example, Lloyd & Bailey 1975; Duda & Schmincke 1978; Becker 1977; Vinx & Jung 1978). Fe-rich green clinopyroxene occurs in Tertiary alkaline rocks from Greenland (K. Brooks, personal communication 1978) and Lloyd & Bailey (1975) describe micaceous, clinopyroxene-rich nodules from Uganda. The South African kimberlite MARID (mica-amphibole-rutile-ilmenite-diopside) suite of xenoliths (Dawson & Smith 1977) may be a less fractionated analogue of the amphibole/apatite suite. The widespread association of this xenolith type with continental (at least) alkaline volcanism may be genetically important as discussed below.

CHEMICAL EVIDENCE FOR MANTLE METASOMATISM

The main chemical evidence for metasomatism of mantle material, apart from the introduction of r.e.e., as outlined below, is the zoning and alteration of original clinopyroxene in Al-augite and Cr-diopside series xenoliths. The close concomitant variation of *Mg* value of coexisting amphibole and clinopyroxene in amphibole/apatite series xenoliths provides a good criterion for establishing whether or not these two minerals were coprecipitated or coequilibrated in a given xenolith. Figure 5 illustrates the tight compositional control of this relationship. The line drawn through the plots of coexisting amphibole/clinopyroxene *Mg* value (from amphibole/apatite suite xenoliths) was calculated by least squares regression

and gives a coefficient of determination of 0.98. Open circles represent Al-augite compositions of two textural types.

First, those joined by dotted lines to amphibole/apatite suite points (solid circles) represent original core Al-augites now partly altered to a more Fe-rich clinopyroxene composition and coexisting with (secondary) amphibole. The amphibole/clinopyroxene *Mg* values plot perfectly along the line for the amphibole/apatite suite compositions, but the Al-augite/amphibole points are significantly displaced because of the higher *Mg* value of the original Al-augite. These chemical data support the introduction of Fe-rich amphibole and clinopyroxene that are compositionally compatible with the amphibole/apatite suite compositions, into pre-existing Al-augite series material. A similar relationship is shown for the Cr-diopside plotted on figure 5 (solid triangle).

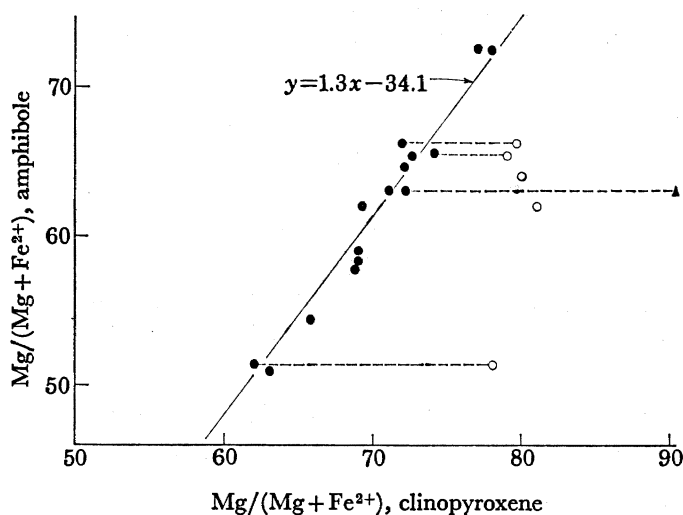


FIGURE 5. *Mg* of coexisting amphiboles and clinopyroxenes. Solid circles are from amphibole/apatite suite assemblages; open circles are Al-augite series clinopyroxene compositions; solid triangle is a clinopyroxene of the Cr-diopside series.

Secondly, the Al-augite compositions not linked to other points (figure 5) represent xenoliths showing ambiguous textural relations between clinopyroxene and amphibole (e.g. figure 4). The clinopyroxenes have a high *Mg* value compared with the coexisting amphibole, suggesting that the amphibole is secondary.

In general the alteration reactions and secondary mineral growth involve introduction of Fe, Ti, P₂O₅ and r.e.e. with l.r.e.e. enrichment. The presence of apatite, amphibole, mica and calcite is evidence for the presence of Cl, F, H₂O and CO₂.

ANALYTICAL PROCEDURES

Representative xenolith types based on mineral assemblages and microprobe data were selected to span the widest chemical variation. Mineral separations were carried out with conventional methods. Final handpicking ensured a purity exceeding 99% except for spinel which may contain minute apatite inclusions. This contamination was corrected for by analysing the spinel for phosphorus and recalculating the analytical results for the spinel.

Neutron activation analyses were carried out by two different techniques. Radiochemical separations were carried out on clinopyroxenes F6 and 45066 and Fen amphibole by using

a method very similar to that described by Brunfelt *et al.* (1974). An instrumental technique was used for the other samples. Small masses (20–150 mg) of the mineral separates, together with element standards and the U.S.G.S. standard rock, BCR-1, were irradiated for about 40 h with a thermal neutron flux of about 1.2×10^{12} neutrons $\text{cm}^{-2} \text{s}^{-1}$. After irradiation, approximately 5 days elapsed before the concentrations of La, Sm and Nd were determined with the use of a GeLi detector (resolution 1.81 keV at 1.33 MeV) and an intrinsic Ge detector (resolution 538 eV at 122 keV). After a further decay period of 1 week the Ge detector was used to determine Ce, Nd, Eu, Tb, Yb and Lu. In all cases appropriate corrections for neutron flux variation, peak interference and half-life were made. Except for K30 biotite, two or more determinations were made for each mineral. In some cases Gd and repeat determinations of Tb and Yb concentrations were made after at least one month had elapsed since irradiation.

The analytical precision for each element was better than 2% standard deviation on the basis of counting statistics, but the standard deviation on the basis of duplicate or more determinations was up to 10% for La, Ce, Nd, Sm and Eu, and up to 20% for Gd, Tb, Yb and Lu. The only exception to these general statements is the K30 biotite where duplicate results were not obtained and the standard deviation on counting statistics was up to 3%.

CHEMICAL COMPOSITIONS AND RESULTS

The major elements of amphibole/apatite suite minerals analysed for r.e.e. and traces are given in table 1 along with the chemical composition of some associated phases in the same xenolith and estimated modal proportions. The *Mg* value for clinopyroxenes ranges from 58 to 72 with concomitant values for coexisting amphiboles and micas. Clinopyroxene (and more rarely amphibole) in contact with the host magma commonly shows titanite rims of quench composition more Mg-rich than the original xenolith clinopyroxene. The variation in chemical composition of all major phases in the amphibole/apatite suite is described in Wass (1979*a*).

In addition to the mineral separates from the Kiama xenoliths, clinopyroxenes, one amphibole and one mica, all inferred to be of high pressure origin associated with alkali basaltic or kimberlitic magmas, were analysed for comparison. Clinopyroxenes chosen range from Fe-rich compositions occurring as megacrysts in basaltic rocks from the Besolles and Montboissier in the Massif Central (FB and F6, figure 7) and 'normal' megacryst compositions from basaltic rocks of the Southern Highlands Province just NW of Kiama (Wass, 1979*b*). An amphibole megacryst from a kimberlitic dyke in the Fen Complex (Griffin & Taylor 1975) was also analysed for r.e.e. (figure 6*a*). The Fe-rich clinopyroxenes from Besolles and Montboissier are compositionally identical to the green Fe-rich clinopyroxenes from the Kiama amphibole/apatite xenoliths such as K24. The Besolles and Montboissier clinopyroxenes are also associated with apatite and spinel.

The r.e.e. concentrations determined are given in table 2 and the chondrite-normalized r.e.e. distributions are illustrated in figures 6 and 7. All values are normalized by using the r.e.e. abundances in chondritic meteorites (Evensen *et al.* 1978), as are the values quoted from other sources.

Apatite (figure 6) consistently shows steep l.r.e.e.-enriched patterns with high chondrite-normalized La/Lu ratios ($(\text{La/Lu})_{\text{c.n.}}$) (48–105). La concentrations show a variation of greater than 2 in the separated apatites (442 $\mu\text{g/g}$ in K41 to 1120 $\mu\text{g/g}$ in K3). This chemical

TABLE 1. MICROPROBE ANALYSES OF MINERALS IN AMPHIBOLE/APATITE INCLUSIONS FROM KIAMA DYKE AND SELECTED CLINOPYROXENES FROM BASALTIC ROCKS

	K24			K41						K30			
	1 cpx.	2 spinel	3 apat.	4 cpx.	5 amph.	6 biot.	7 spinel	8 ilm.	9 apat.	10 cpx.	11 amph.	12 biot.	13 apat.
SiO ₂	49.5	2.19	0.26	48.3	38.89	35.5	0.03	0.03	0.27	46.5	39.0	35.5	0.38
TiO ₂	0.88	22.44	n.d.	2.05	5.37	6.4	19.8	51.0	n.d.	2.34	5.19	7.42	n.d.
Al ₂ O ₃	4.05	3.96	n.d.	6.94	13.4	15.8	3.44	0.20	n.d.	7.5	14.1	15.3	n.d.
Cr ₂ O ₃	n.d.	n.d.	n.d.	n.d.	n.d.	n.d.	n.d.	n.d.	n.d.	n.d.	n.d.	n.d.	n.d.
Fe ₂ O ₃	4.32	40.98	—	—	—	2.41	—	—	—	—	3.94	2.24	—
FeO	9.20	30.02	—	—	—	14.62	—	—	—	—	10.16	15.41	—
FeO†	—	—	0.29	9.50	14.3	—	72.0	42.7	0.36	9.0	—	—	0.27
NiO	n.d.	n.d.	n.d.	n.d.	n.d.	n.d.	n.d.	n.d.	n.d.	n.d.	n.d.	n.d.	n.d.
MnO	0.37	0.68	n.d.	0.23	0.26	0.21	0.82	0.76	n.d.	0.30	0.27	0.11	n.d.
MgO	10.3	0.42	0.15	10.9	10.2	12.3	0.20	5.54	0.22	10.9	10.1	10.8	0.14
CaO	20.7	0.22	53.3	21.2	11.6	n.d.	0.08	0.10	53.8	22.5	11.6	n.d.	53.6
Na ₂ O	1.26	n.d.	n.d.	1.12	2.31	0.68	n.d.	n.d.	n.d.	1.25	2.29	0.63	n.d.
K ₂ O	n.d.	n.d.	n.d.	n.d.	2.11	8.40	n.d.	n.d.	n.d.	n.d.	2.06	8.42	n.d.
P ₂ O ₅	—	—	40.5	—	n.d.	—	—	—	41.2	—	n.d.	—	40.3
F	—	—	1.42	—	0.12	—	—	—	2.00	—	0.13	—	2.08
Cl	—	—	0.23	—	0.04	—	—	—	0.18	—	0.02	—	0.22
Total	100.6	100.9	96.2	100.2	98.6	96.3	96.4	100.3	98.0	100.3	98.9	95.8	97.0
Mg	58.4	—	—	67.2	56.0	56.6	—	—	—	68.3	56.8	52.4	—
(Mg + Fe)†	58.4	—	—	67.2	56.0	56.6	—	—	—	68.3	56.8	52.4	—

Where reported, the FeO/Fe₂O₃ was determined colorimetrically with the use of 2,2'-dipyridyl reagent.
n.d., not detected.

† Total Fe as FeO.

variation is consistent with the occurrence of crystal fractionation as indicated also by the sequential Fe-enrichment among the xenoliths (see Introduction). La values are 1800–4600 times chondrite, a little lower than those for apatites in ijolite associated with carbonatite in Ontario (Cullers & Medaris 1977) but with a similar chondrite-normalized pattern. Apatites from carbonatites of West Siberia and the Kola Province (Balashov & Pozharitskaya 1968) similarly show steep, l.r.e.e.-enriched patterns with high (La/Lu)_{c.n.} ratios. Apatites from the Oka carbonate complex (Eby 1975) show extreme l.r.e.e. enrichment with La up to 43000 times chondrite. Steeply inclined patterns are again typical but negative Eu anomalies are present, unlike the Kiama apatite. Prins (1973) records La and Ce for four apatites from African carbonatites. La varies from about 240–3000 times chondrite.

Apatite has the highest concentration of r.e.e. of all minerals from the Kiama amphibole/apatite suite and also has the greatest relative enrichment in l.r.e.e. Therefore, the occurrence of significant modal apatite will give a steep l.r.e.e. pattern to the whole rock.

Clinopyroxene (K24, figure 6c) shows a pattern of slight overall l.r.e.e. enrichment with a concave downward curve from La to Sm. However, the relative concentrations of r.e.e. are much higher (La 100 times chondrite) compared with 'normal' high-pressure basaltic megacrysts (La 7–13 times chondrite), as shown in figure 7. The green Fe-rich clinopyroxenes from Besolles (FB) and Montboissier (F6) are identical in ranges of major elements with the Fe-rich clinopyroxenes from the Kiama amphibole/apatite xenoliths (such as K24, table 1). Both FB and MB clinopyroxenes have r.e.e. patterns similar to K24 (figures 6c and 7) and both are also enriched in r.e.e. compared with the 'normal' megacrysts from Riley's Peak,

APATITE-RICH XENOLITHS

339

TABLE 1. (cont.)

	K3			K13A1					K	FB	F6(1)	45066A
	14	15	16	17	18	19	20	21				
	cpx.	amph.	ilm.	cpx.	amph.	spinel	ilm.	apat.	apat.	cpx.	cpx.	cpx.
SiO ₂	47.5	38.8	0.10	46.2	39.7	0.14	0.05	0.30	0.19	47.1	48.2	48.3
TiO ₂	2.10	6.11	51.2	2.61	4.07	21.3	51.2	n.d.	n.d.	1.83	1.72	1.48
Al ₂ O ₃	7.40	14.1	0.25	8.07	14.0	6.23	0.31	n.d.	n.d.	6.70	6.21	8.57
Cr ₂ O ₃	n.d.	n.d.	n.d.	n.d.	n.d.	n.d.	n.d.	n.d.	n.d.	n.d.	n.d.	0.17
Fe ₂ O ₃	—	4.4	—	—	—	—	—	—	—	0.7	—	—
FeO	—	6.3	—	—	—	—	—	—	—	11.0	—	—
FeO†	8.12	—	42.0	7.86	12.2	67.3	41.0	0.24	0.35	—	10.0	5.93
NiO	n.d.	n.d.	n.d.	n.d.	n.d.	n.d.	n.d.	n.d.	n.d.	n.d.	n.d.	n.d.
MnO	n.d.	n.d.	0.57	0.16	0.13	0.63	0.74	0.06	n.d.	0.22	0.22	n.d.
MgO	11.0	12.6	6.20	11.2	12.0	0.07	6.17	0.12	0.01	9.72	10.5	13.5
CaO	22.6	12.3	0.20	23.3	12.2	0.05	0.07	54.2	53.2	21.4	21.8	20.6
Na ₂ O	1.44	2.07	n.d.	0.76	2.40	n.d.	n.d.	n.d.	n.d.	1.21	1.30	0.85
K ₂ O	n.d.	2.18	n.d.	n.d.	1.67	n.d.	n.d.	n.d.	n.d.	n.d.	n.d.	n.d.
P ₂ O ₅	—	—	—	—	—	—	—	41.4	40.9	—	—	—
F	—	—	—	—	—	—	—	2.52	1.63	—	—	—
Cl	—	—	—	—	—	—	—	0.23	0.15	—	—	—
Total	100.2	98.9	100.4	100.2	98.3	95.7	99.5	99.1	96.4	99.9	99.9	99.4
Mg	70.7	68.6	—	71.8	63.7	—	—	—	—	59.9	65.2	80.2
(Mg+Fe)†	70.7	68.6	—	71.8	63.7	—	—	—	—	59.9	65.2	80.2

Estimated modes of inclusions and localities

K24: Fe-rich clinopyroxene 50 %, apatite 30 %, spinel 20 %, accessory carbonate, sulphides.

K41: Kaersutite 40 %, clinopyroxene 20 %, apatite 20 %, biotite 10 %, spinel 10 %, accessory carbonate, sulphides, ilmenite.

K30: Kaersutite 30 %, clinopyroxene 30 %, apatite 25 %, biotite 10 %, spinel 5 %, accessory sulphides.

K3: Kaersutite 95 %, ilmenite 3 %, clinopyroxene 2 %, accessory carbonate, sulphides.

K13A1: Clinopyroxene 42 %, titaniferous pargasite 28 %, apatite 20 %, ilmenite and opaque spinel 10 %, accessory sulphides, carbonate.

K: Apatite 50 %, opaque spinel 50 %, accessory sulphides, carbonate, mica.

All K numbers are specimens from the nepheline basanite dyke in Bombo Quarry, N of Kiama, NSW.

FB is a megacryst in basaltic host from Besolles, Massif Central.

F6(1) is a megacryst in basaltic host from Montboissier, Massif Central.

45066A is a megacryst in nepheline basanite from Riley's Peak, Southern Highlands, NSW.

TABLE 2. RARE EARTH ELEMENT CONCENTRATIONS (micrograms per gram)
IN SEPARATED MINERALS

	K24			K41	K30			K3		K	FB
	1	2	3		4	5	6	7	8		
	cpx.	spinel†	apat.	apat.	amph.	biot.	apat.	amph.	apat.	apat.	cpx.
La	26.4	8.3	770	442	20.8	13.7	530	14.1	1120	1110	31.6
Ce	84	19.0	1860	930	65	34	1300	47.2	2180	2320	87
Nd	52.7	10.1	796	416	40.6	6.6	631	31.5	824	1023	50.8
Sm	11.9	1.78	145	86	10.4	1.9	111	8.3	134	165	12.0
Eu	3.71	0.56	37.3	21.0	2.90	0.33	31.3	2.4	36.9	43.1	3.59
Gd	—	—	—	—	—	—	—	7.1	—	—	—
Tb	1.39	0.27	13.0	8.68	1.21	0.20	12.1	1.00	14.6	13.4	1.32
Yb	2.0	0.42	9.8	6.23	1.6	0.71	10.6	1.31	10.4	11.0	2.85
Lu	0.35	0.11	1.10	0.95	0.25	—	1.12	0.20	1.65	1.10	0.51
(La/Lu) _{c.n.}	7.8	7.7	73	48	8.7	—	49	7.3	70	105	6.4

† K24 spinel results corrected for apatite contamination estimated from presence of 0.05 % P₂O₅.

with FB r.e.e. abundances being almost exactly the same as those of the Kiama K24 clinopyroxene. The increase in r.e.e. concentration from Riley's Peak through Montboissier to Besolles clinopyroxenes is followed by a decreasing *Mg* value from approximately 80 through 65 to 60. The Riley's Peak megacrysts are in the usual compositional range for high-pressure megacrysts from alkali basaltic rocks (Wass 1979*b*; Irving 1974). The Fe-rich clinopyroxenes (K24, FB, F6) all reflect crystallization from a fluid rich in r.e.e. and form a distinct group recognizable by higher r.e.e. abundances.

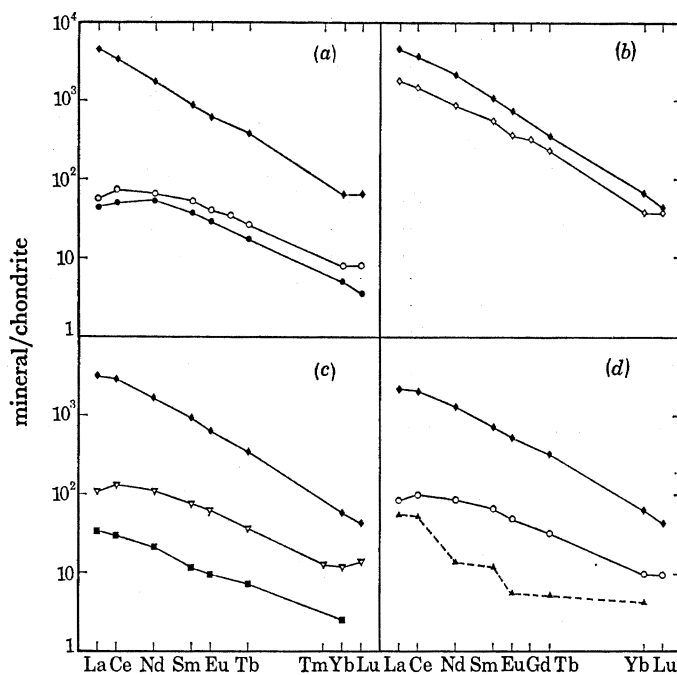


FIGURE 6. (a) Rare earth element contents of K3 minerals normalized to chondrites, with Fen amphibole (solid circles) for comparison. (b) Rare earth element contents of K apatite (solid diamonds) and K41 apatite (open diamonds) normalized to chondrites. (c) Rare earth element contents of K24 minerals normalized to chondrites. (d) Rare earth element contents of K30 minerals normalized to chondrites. \blacklozenge , \diamond , Apatite; \bullet , \circ , amphibole; ∇ , pyroxene; \blacksquare , spinel; \blacktriangle , biotite.

Clinopyroxene r.e.e. patterns in carbonatite complexes show a variety of r.e.e. abundances and chondrite-normalized patterns. The Seabrook Lake ijolite clinopyroxene has a straight l.r.e.e.-enriched pattern with $(La/Lu)_{c.n.}$ about 30 (Cullers & Medaris 1977), while the Oka carbonatite complex clinopyroxenes show a variation from a pattern similar to those of this study but ranging from comparable abundances to La concentrations of 650 times chondrite to patterns with lower abundances and large positive Eu anomalies (Eby 1975).

Comparison with probable 'normal' upper mantle Cr-diopside type clinopyroxenes can be made by using data of Frey & Green (1974) and Frey & Prinz (1978). Both r.e.e. abundances and patterns show a wide variation. Abundances range from about 90 to 4 times chondrite for La. Patterns for higher abundances show significant l.r.e.e. enrichment often with concave downward curvature for l.r.e.e. Relatively flat, slight enrichment in high atomic number rare earth elements (h.r.e.e.) or slight l.r.e.e. enrichment characterize the patterns for lower abundances.

Shimizu (1975) shows two r.e.e. abundance groups for garnet lherzolites from kimberlites. One group with higher r.e.e. concentrations (Ce 30–40 times chondrite) has a granular

microstructure, the other (Ce 5–11 times chondrite) has a sheared microstructure. Both groups show l.r.e.e.-enriched patterns (more pronounced for the granular xenoliths) with a concave downward curvature for the l.r.e.e.

Amphibole. K30 (figure 6d) and K3 (figure 6a) also shows slight r.e.e. enrichment, $(La/Yb)_{c.n.}$ being about 8 with a shallow sigmoidal curve. R.e.e. concentrations are slightly lower than for K24 clinopyroxene but are twice the chondritic abundance (but with identical pattern) as an amphibole megacryst from the Fen kimberlitic dyke shown for comparison (figure 6a).

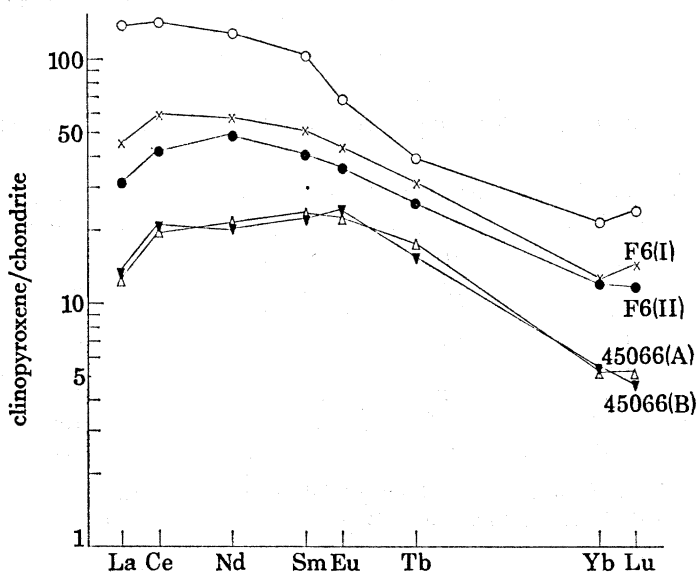


FIGURE 7. Rare earth element contents of clinopyroxenes occurring in high-pressure inclusions and as megacrysts in alkali basaltic rocks. Open circles are FB clinopyroxene.

Spinel. K24 (figure 6c) follows the general l.r.e.e. enrichment trend of all amphibole/apatite inclusion minerals. Chondrite-normalized r.e.e. abundances are low compared with a magnetite in ijolite (Cullers & Medaris 1977), which has La about 450 times chondrite. However, the r.e.e. concentrations of the K24 spinel are of a magnitude that is expected if the partition coefficients (magnetite/dacitic matrix) determined by Schock (1977) are applicable to this system. The calculated r.e.e. contents of the parent magma are similar to those calculated from the K24 apatite when the partition coefficients by Nagasawa (1970) for apatite–dacite magma systems are used.

The general absence of europium anomalies from the apatites, amphiboles and clinopyroxenes is important in suggesting that the $Eu^{2+}:Eu^{3+}$ ratio in the parent magma was very low. An anomaly would be expected in the apatite, on the basis of established partition coefficients for the r.e.e. (see, for example, Nagasawa 1970) and from considerations of its structure if significant Eu^{2+} was present (Eby 1975).

PARTITION COEFFICIENTS

R.e.e. partition coefficients for certain mineral pairs of the amphibole–apatite xenoliths are given in table 3. As indicated above, the K24 values for apatite–spinel are comparable with those calculated from apatite–liquid and spinel–liquid data that have been published

(Nagasawa 1970; Schock 1977). Similarly, the partition coefficients for the K24 apatite-clinopyroxene pair are similar to those for the same mineral pair of an ijolite from the Seabrook Lake Complex (Cullers & Medaris 1977; see table 3). These results suggest that K24 has crystallized under equilibrium conditions. However, the r.e.e. partition coefficients for the apatite-amphibole pair (K30 and K3) vary by up to a factor of 3 (La) and are different from coefficients determined for an apatite-arfvedsonite coexisting pair from the Kangerdlugssuaq intrusion, East Greenland (Henderson 1980). Hence, K30 and K3 do not appear to be equilibrium assemblages, but more data are required before the nature and extent of the disequilibrium may be ascertained.

TABLE 3. RARE EARTH ELEMENT PARTITION COEFFICIENTS FOR MINERAL PAIRS

	K24		Ijolite 19† apat./cpx.	K30 apat./amph.	K3 apat./amph.	EG2857‡ apat./amph.
	apat./spinel	apat./cpx.				
La	93	29	21	25	79	170
Ce	98	22	18	20	46	170
Nd	79	15	—	16	26	92
Sm	81	12	13	11	16	74
Eu	67	10	12	11	15	67
Tb	48	9.4	12	10	15	68
Yb	23	5.0	6.3	6.5	7.9	6.6
Lu	10	3.1	4.5	4.5	8.2	3.1

† Seabrook Lake complex, Ontario (Cullers & Medaris 1977).

‡ Kangerdlugssuaq intrusion, East Greenland (Henderson 1980).

Calculated partition coefficients of mineral/host xenolith data indicate that the host rock is unlikely to represent the liquid composition from which the analysed apatites, clinopyroxenes, amphiboles, spinels and mica crystallized. This supports the concept that the different amphibole/apatite suite assemblages represent crystallization at different stages in a differentiation sequence (Wass 1979a).

A decreasing preference of apatite for r.e.e. with increasing atomic number relative to clinopyroxene is shown in figure 8 in a plot of apatite:clinopyroxene r.e.e. ratios. Two apatite-clinopyroxene pairs are plotted: K24 apatite-clinopyroxene and K apatite-FB clinopyroxene. The latter plot was made because FB apatite could not be separated and it is important to attempt to establish the relation of the Besolles Fe-rich clinopyroxene with the Kiama equivalent. The use of K apatite was justified because (i) Fe-rich green clinopyroxene compositionally similar to the Besolles FB clinopyroxene occurs in layers in Kiama apatite-spinel xenoliths similar to K, and (ii) the Besolles FB clinopyroxene commonly occurs associated with apatite and spinel similar in major element composition to those in the Kiama xenolith K. The close correspondence of the two curves in figure 11 does suggest a close relationship between the Besolles and Kiama Fe-rich clinopyroxenes. The l.r.e.e. part of the curve closely corresponds with that for soda pyroxene sovite apatite-clinopyroxene pairs from the Oka carbonatite complex (Eby 1975) but the latter shows a marked preference of pyroxene for Eu.

Figure 9 shows the r.e.e. values of possible liquids in equilibrium with K24 clinopyroxene and apatite. The shaded area represents the range of possible liquids by using maximum and minimum partition coefficients from Schnetzler & Philpotts (1970) and solid circles give a liquid by using the values from Tanaka & Nishizawa (1975). The latter was chosen from the data for Ca pyroxene-liquid coefficients in Irving (1978) to represent a high-pressure value.

The partition coefficients for r.e.e. in apatite are also from Irving (1978) as calculated for apatite in a kimberlitic host. The calculated possible liquids (figure 9) suggest that the parent liquid for K24 clinopyroxene and apatite may lie in the range with La 340–800 times chondrite with $(La/Lu)_{c.n.}$ about 30. The pattern shows l.r.e.e. enrichment with an abundance range overlapping the values for carbonatites and kimberlites (see, for example, Mitchell & Brunfelt 1975*a, b*; Frey *et al.* 1977; Cullers & Medaris 1977; Fesq *et al.* 1975).

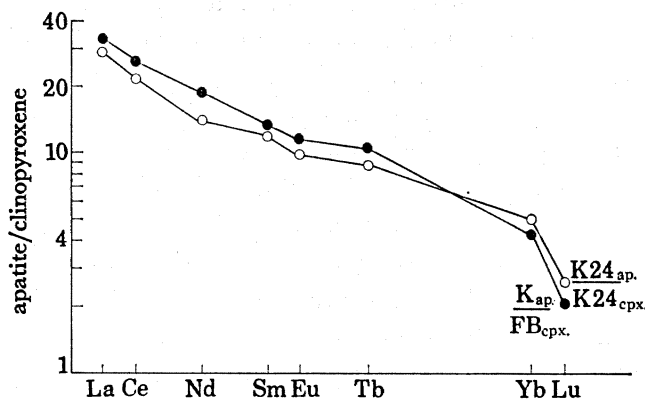


FIGURE 8. Rare earth element abundance ratios for selected apatite-clinopyroxene pairs.

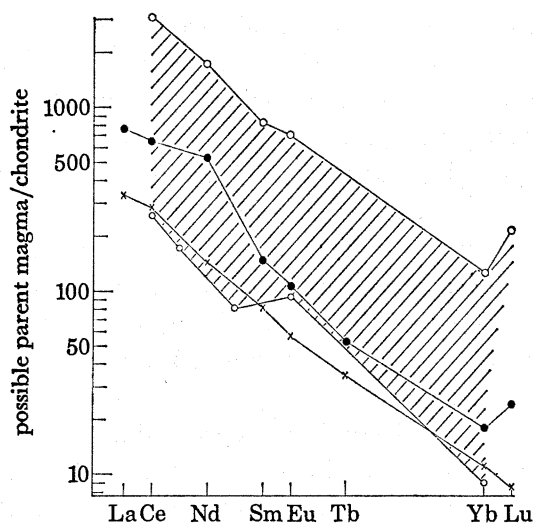


FIGURE 9. Estimated possible liquid compositions that may have equilibrated with FB apatite and clinopyroxene. Shaded area between open circles represents range of values calculated by using clinopyroxene partition coefficients from Schnetzler & Philpotts (1970). Solid circles represent liquid calculated by using clinopyroxene partition coefficient of Tanaka & Nishizawa (1975). Crosses represent liquid calculated by using apatite partition coefficient of Irving (1978).

DISCUSSION

Upper mantle metasomatism

The high r.e.e. concentrations of apatite, clinopyroxene, amphibole, biotite and spinel mineral separates from the Kiama amphibole/apatite suite xenoliths are consistent with crystallization from r.e.e.-abundant and l.r.e.e.-enriched liquid such as a kimberlitic/carbonatitic fluid. The higher r.e.e. concentrations associated with increasing Fe content

of clinopyroxenes (decreasing Mg value) are also consistent with the amphibole/apatite series xenoliths representing a fractional crystallization sequence. An upper mantle origin is indicated by the veining and alteration of associated Cr-diopside and Al-augite composition, interpreted as mantle wall-rock.

These concepts suggest that there are volatile-rich fluids, rich in incompatible elements including r.e.e., which could be a source for metasomatic alteration of upper mantle material. Frey & Green (1974) and Frey & Prinz (1978) show that upper mantle material consists of two components: an 'A' component which is upper mantle residual after some partial melting and a liquid 'B' component, rich in incompatible elements, which has migrated upwards (probably from the low-velocity zone) and thereby introduced the incompatible elements into component A, dominantly by crystallization of clinopyroxene, amphibole and mica. The fluid from which the apatite/amphibole xenoliths crystallized would be rich in component B although with a greater Fe content because of its fractionated history. Frey *et al.* (1978) suggest that the upper mantle source rocks beneath northwestern Victoria, modelled on r.e.e. contents of the basaltic products, are l.r.e.e. enriched. The addition of apatite with the r.e.e. patterns of K and K24 would impose such a pattern on upper mantle rocks. In subsequent partial fusions apatite will melt early and probably completely (Frey *et al.* 1978; Sun & Hanson 1975*a*).

A parallel relation of incompatible element enrichment is evident in granular compared with sheared garnet lherzolites from South Africa (Shimizu 1975). The granular garnet lherzolites are analogous to the spinel lherzolites enriched in component B of Frey & Green (1974) and could result from metasomatism of original upper mantle by fluids similar to those that are the parent of the amphibole/apatite suite assemblages.

Many mantle lherzolites contain apatite, amphibole or mica, commonly interstitial and secondary in origin (see, for example, Frey & Green 1974; Best 1974; Dawson & Smith 1977). These phases closely correspond with the Kiama amphibole/apatite suite constituents. Sun & Hanson (1975*a, b*) consider, on the basis of Ce:P₂O₅ ratios, that apatite is an important and ubiquitous phase in the source region for alkali basaltic magmas but is rarely residual. They also suggest that mica as well as apatite is abundant and, unlike apatite, is residual in the mantle source for nephelinites. Lloyd & Bailey (1975) interpret xenoliths in alkaline rocks from the Eifel region and southwest Uganda as representing metasomatized upper mantle, incorporating Fe-rich clinopyroxene, amphibole, mica and apatite. They consider that this metasomatism could account for the chemical characteristics of alkaline volcanism. As outlined above, inclusions in alkali basaltic rocks consisting of mineral assemblages analogous to those of the amphibole/apatite suite are found in many alkaline provinces (so far all continental, but this may simply be a sampling problem) from geographically widely separated areas. Primary and near-primary alkali basaltic (and kimberlitic) magmas have very similar major element and r.e.e. distributions (l.r.e.e. enriched), irrespective of location (Schwarzer & Rogers 1974; Sun & Hanson 1975*a, b*; Kay & Gast 1973; Frey *et al.* 1977, 1978). Frey *et al.* (1978) suggest a model upper mantle beneath western Victoria which has l.r.e.e. concentrations about 8–12 times chondrite and h.r.e.e. concentrations about 3–4 times chondrite. This model adequately accounts for the r.e.e. abundances of the western Victoria basaltic province.

All of these data are consistent with a common process of enrichment in incompatible elements of upper mantle material which is then geochemically suitable as a source of alkaline

magma on partial melting. The widespread evidence of amphibole/apatite suite minerals in mantle and alkali basaltic rocks and the l.r.e.e.-enriched nature shown by minerals of this suite from Kiama and the Massif Central strongly suggest that the parental fluid for the amphibole/apatite assemblages is a common association with alkaline volcanism and may be a prerequisite factor.

Origin of the parental magma for the amphibole/apatite suite

The characteristics of this parental fluid would be a low concentration of silica and high concentrations of Ti, incompatible elements and volatiles including CO₂, H₂O, Cl and F. Fractional crystallization of such a melt would result in residual kimberlite and carbonatite (Wyllie & Huang 1975). The origin of this liquid must lie deep in the upper mantle and may represent volatile-rich melting in the low velocity zone (Frey *et al.* 1978; Wyllie 1977). Upward percolation of this fluid may effect metasomatism and/or culminate in volcanic activity. If it cannot escape the upper mantle for some reason (such as lowering of temperature, increasing viscosity or lack of sufficient volume to necessitate continued ascent) the magma may fractionate within the upper mantle, producing veins and lenses equivalent to the amphibole/apatite series assemblages. Loubet *et al.* (1972) and Balashov *et al.* (1964) suggest that h.r.e.e. carbonate complexes are more stable than l.r.e.e. carbonate complexes, so that crystallization from a carbonate-rich fluid will create or enhance l.r.e.e. enrichment, with h.r.e.e. enrichment in any associated CO₂-rich gaseous phase.

Part of this study was carried out while S.Y.W. was visiting the British Museum (Natural History) and University of London Reactor Centre. Dr A. C. Bishop and Mr M. Kerridge kindly made facilities available at these two institutions respectively. The hospitality of the Mineralogisk Museum, Oslo, through Dr W. Griffin, the use of the Neutron Activation Laboratory there, and the help and expertise of Dr A. Brunfelt are also gratefully acknowledged. Electron microprobe time at the Smithsonian Institute (Washington) and the assistance of Mr G. Pooley at Macquarie University facilitated mineral analyses for major elements. S.Y.W. received grant support for parts of this study from the Australian Research Grants Committee and Macquarie University Research Grant Scheme.

REFERENCES (Wass *et al.*)

- Aoki, K. & Shiba, I. 1973 *Lithos* **6**, 41–51.
 Babkine, J., Conquere, F. & Vilminot, J. C. 1968 *Bull. Soc. fr. Minér. Cristallogr.* **91**, 141–150.
 Balashov, Y. A., Bronov, A., Migdisov, A. A. & Turanskaya, N. U. 1964 *Geochem. int.* **5**, 951–980.
 Balashov, Y. A. & Pozharitskaya, L. K. 1968 *Geochem. int.* **5**, 271–288.
 Becker, A. J. 1977 *Contr. Miner. Petr.* **65**, 45–52.
 Best, M. G. 1974 *J. geophys. Res.* **79**, 2107–2113.
 Best, M. G. 1975 *J. Petr.* **16**, 212–236.
 Brunfelt, A. O., Roelandts, I. & Steinnes, E. 1974 *Analyst* **99**, 277–284.
 Conquéré, F. 1971 *Contr. Miner. Petr.* **33**, 32–61.
 Cullers, R. L. & Medaris Jr, G. 1977 *Contr. Miner. Petr.* **65**, 143–153.
 Dawson, J. B. & Smith, J. V. 1977 *Geochim. cosmochim. Acta* **41**, 309–323.
 Duda, A. & Schmincke, H.-V. 1978 *Neues Jb. Miner. Abh.* **132**, 1–33.
 Eby, G. N. 1975 *Geochim. cosmochim. Acta* **39**, 597–620.
 Embey-Isztin, A. 1976 *Earth planet. Sci. Lett.* **31**, 297–304.
 Evensen, N. M., Hamilton, P. J. & O'Nions, R. K. 1978 *Geochim. cosmochim. Acta* **42**, 1199–1212.
 Fesq, H. W., Kable, E. J. D. & Gurney, J. J. 1975 *Phys. Chem. Earth* **9**, 687–708.

- Frey, F. A., Ferguson, J. & Chappell, B. W. 1977 In *Ext. Abstr. 2nd Int. Kimb. Conf.*, Santa Fe.
- Frey, F. A. & Green, D. H. 1974 *Geochim. cosmochim. Acta* **38**, 1023–1059.
- Frey, F. A., Green, D. H. & Roy, S. D. 1978 *J. Petr.* **19**, 463–513.
- Frey, F. A., & Prinz, M. 1978 *Earth planet. Sci. Lett.* **38**, 129–176.
- Griffin, W. L. & Taylor, P. N. 1975 *Phys. Chem. Earth* **9**, 163–178.
- Henderson, P. 1980 *Contr. Miner. Petr.* (In the press.)
- Irving, A. J. 1974 *Bull. geol. Am.* **85**, 1503–1514.
- Irving, A. J. 1978 *Geochim. cosmochim. Acta* **42**, 743–770.
- Irving, A. J. 1980 *Am. J. Sci.* (In the press.)
- Kay, R. W. & Gast, P. W. 1973 *J. Geol.* **81**, 653–682.
- Lloyd, F. E. & Bailey, D. K. 1975 *Phys. Chem. Earth* **9**, 389–416.
- Loubet, M. Bernat, M., Javoy, M. & Allègre, C. 1972 *Earth planet. Sci. Lett.* **14**, 226–232.
- Mitchell, R. H. & Brunfelt, A. O. 1975 *a Contr. Miner. Petr.* **52**, 247–259.
- Mitchell, R. H. & Brunfelt, A. O. 1975 *b Phys. Chem. Earth* **9**, 671–686.
- Nagasawa, H. 1970 *Earth planet. Sci. Lett.* **9**, 359–364.
- Prins, P. 1973 *Lithos* **6**, 133–144.
- Schnetzler, C. C. & Philpotts, J. A. 1970 *Geochim. cosmochim. Acta* **34**, 331–340.
- Schock, H. H. 1977 *J. Radioanal. Chem.* **8**, 327–340.
- Schwarzer, R. R. & Rogers, J. J. W. 1974 *Earth planet. Sci. Lett.* **23**, 286–296.
- Shimizu, N. 1975 *Earth planet. Sci. Lett.* **25**, 26–32.
- Sun, S.-S. & Hanson, G. N. 1975 *a Contr. Miner. Petr.* **52**, 77–106.
- Sun, S.-S. & Hanson, G. N. 1975 *b Geology* **3**, 297–302.
- Tanaka, T. & Nishizawa, O. 1975 *Geochem. J.* **9**, 161–166.
- Vinx, R. & Jung, D. 1978 *Contr. Miner. Petr.* **65**, 135–142.
- Wass, S. Y. 1979 *a In Proc. 2nd Int. Kimb. Conf.*, vol. **2**, pp. 366–373. A.G.U.
- Wass, S. Y. 1979 *b Lithos* **12**, 115–132.
- Wass, S. Y. & Irving, A. J. 1976 *Xenmeg: a catalogue of occurrences of xenoliths and megacrysts in volcanic rocks of eastern Australia*. (441 pages.) Sydney: Australian Museum.
- Wass, S. Y. & Rogers, N. W. 1980 In preparation.
- Wilkinson, J. F. G. 1975 *Contr. Miner. Petr.* **51**, 235–262.
- Wilshire, H. G. & Shervais, J. W. 1975 *Phys. Chem. Earth.* **9**, 257–272.
- Wilshire, H. G. & Trask, N. J. 1971 *Am. Miner.* **56**, 240–255.
- Wyllie, P. J. 1977 *J. Geol.* **85**, 187–207.
- Wyllie, P. J. & Huang, W. L. 1975 *Geology* **3**, 621–624.



FIGURE 1. Bladed amphibole and apatite replacing clinopyroxene from original Al-augite type xenolith. Width of field of view: 3.5 mm.

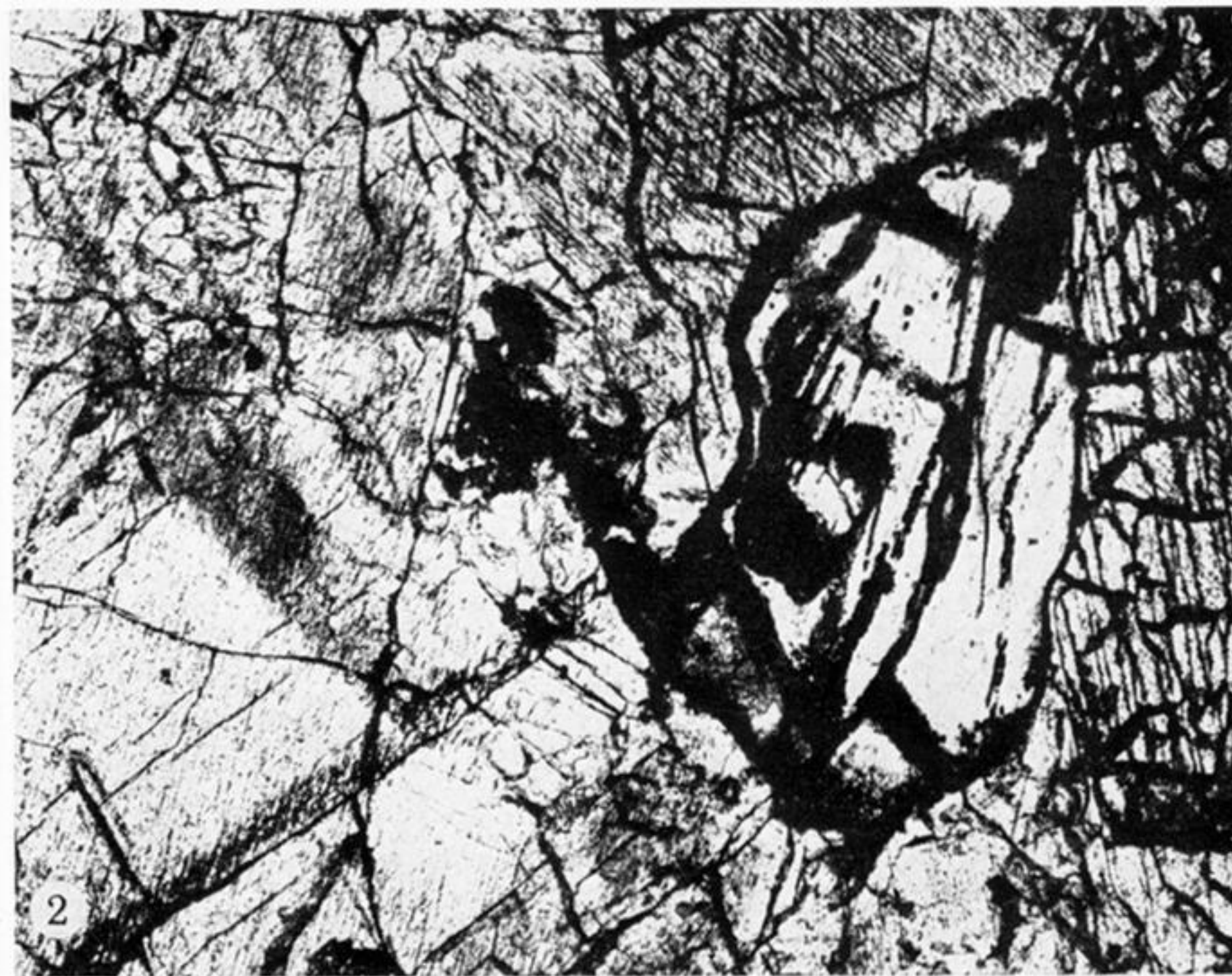


FIGURE 2. Altered Al-augite type xenolith. Olivine is pseudomorphed by carbonate, original clinopyroxene is clouded with opaques and altered to Fe-rich clinopyroxene at grain boundaries. Width of field of view: 3.5 mm.

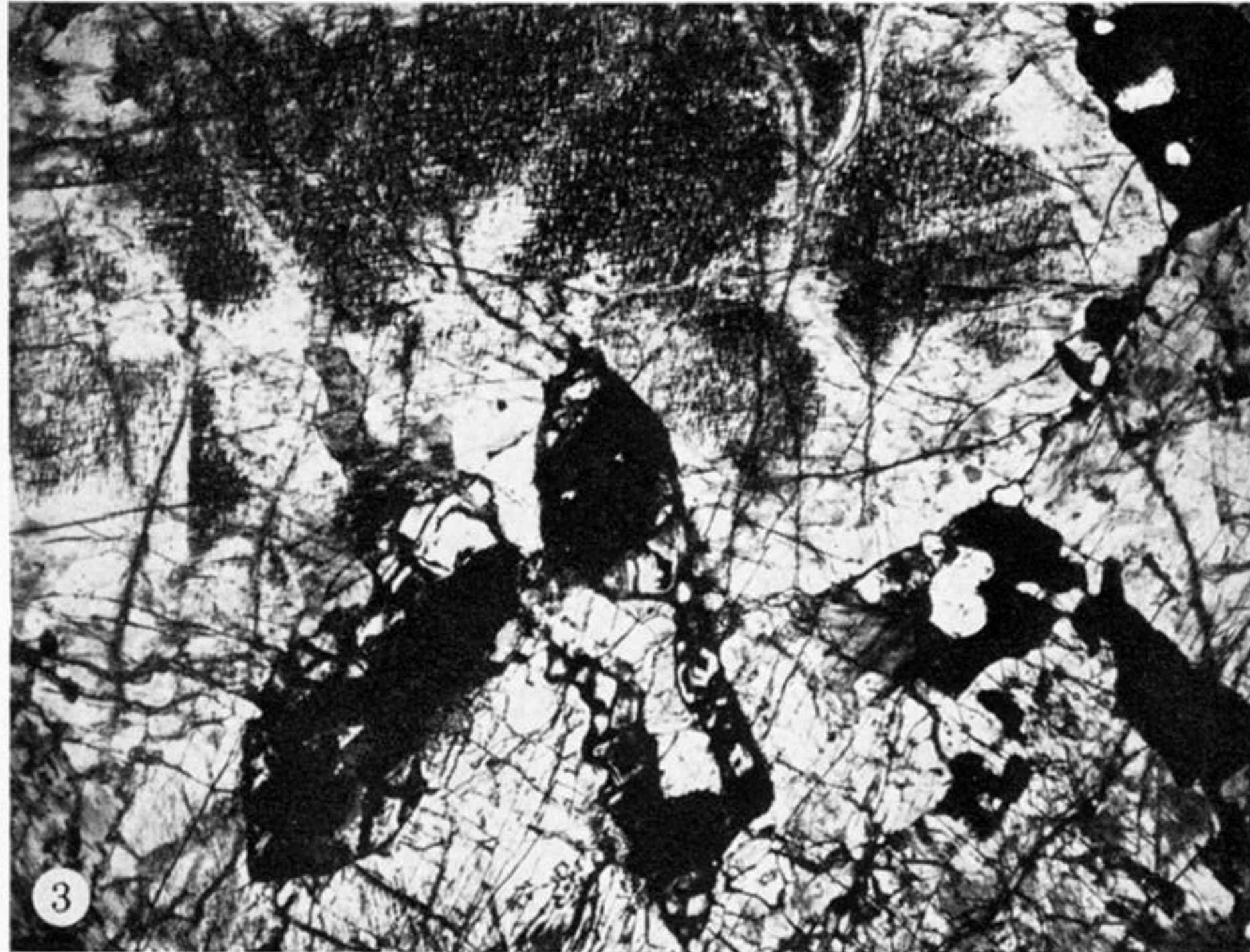


FIGURE 3. Altered Al-augite type xenolith showing altered olivine and clinopyroxene. Width of field of view: 3.5 mm.

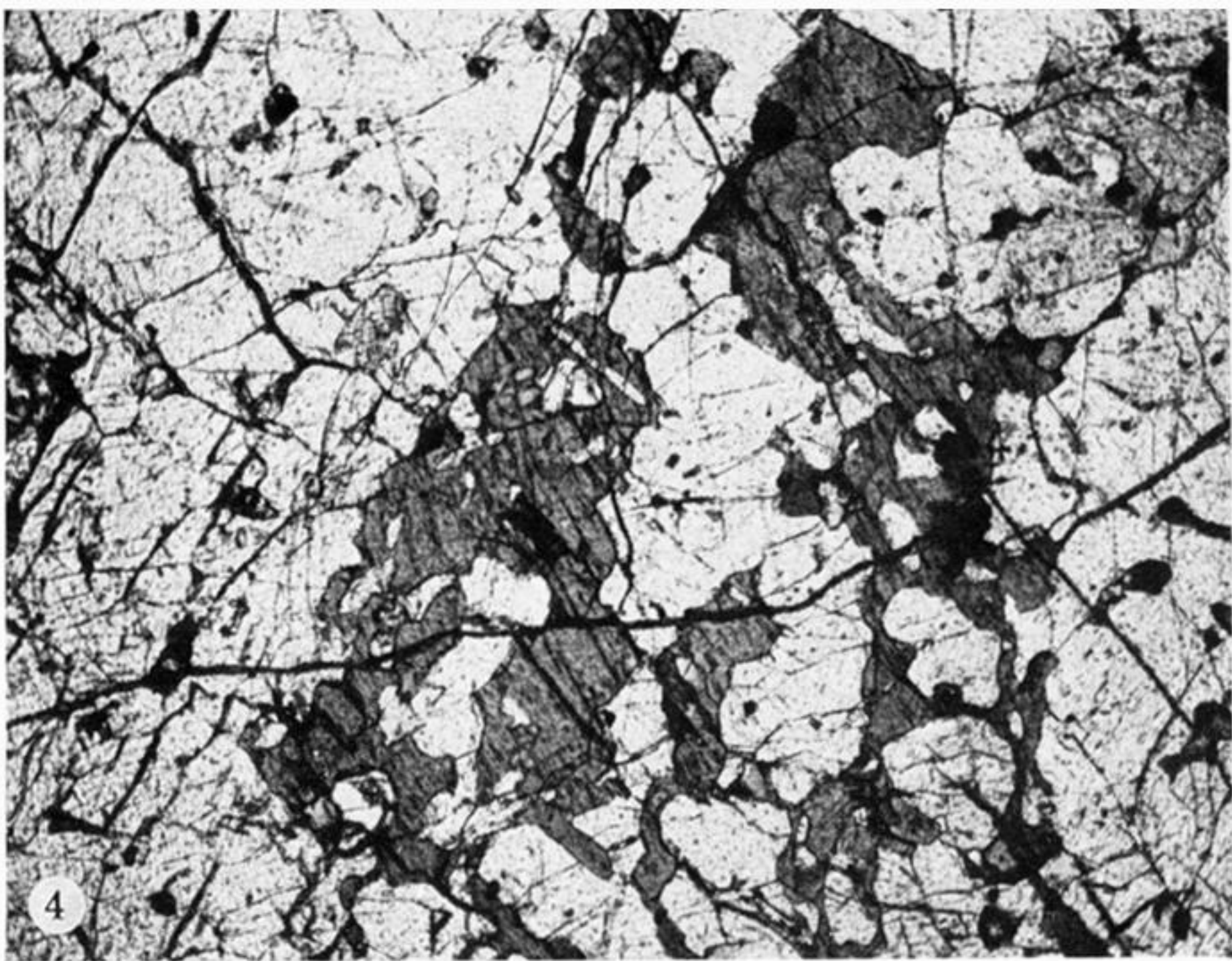


FIGURE 4. Intergrowth of amphibole and clinopyroxene. Width of field of view: 3.5 mm.